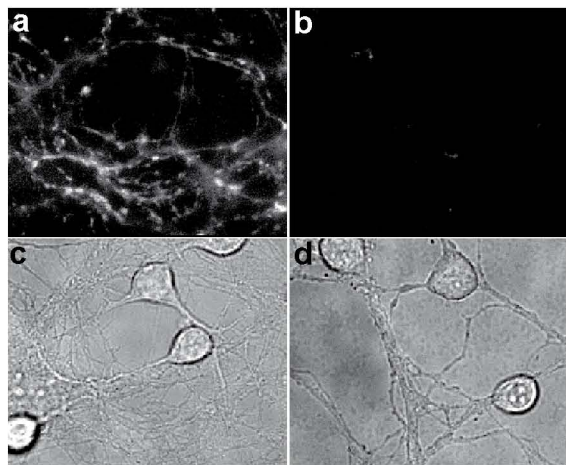


Fig. S1- TetradecylTriMethylAmmonium Bromide (MiTMAB™) completely abolished synaptic vesicle endocytosis after stimulation. FM1-43 images prior to the unloading of 7 DIV cerebellar granule cells labeled in the absence (Aa) or in the presence (Ab) of MiTMAB (5 μ M, 10min) at normal (1.3 mM CaCl₂) Ca²⁺ concentrations. Ac and Ad represent phase contrast images of cells in control and MiTMAB, respectively. B, shown are examples of individual unloading kinetics in control and in the presence of MiTMAB. Note the higher noise level in MiTMAB experiments due to the lower signal to noise ratio. C, Mean initial fluorescence (a.u.) in control and MiTMAB-treated synaptic boutons, ($p \leq 0.01$; ANOVA). D, Frequency histogram of FM1-43 initial fluorescence in control and MiTMAB-treated cells. (E) Cumulative probability of the initial FM1-43 fluorescence measured prior to unloading with 50 mM KCl in the presence or absence of MiTMAB (5 μ M, 10 minutes) at normal (1.33 mM) CaCl₂ concentrations.

A Control MiTMAB, 5 μ M



B Control MiTMAB, 5 μ M

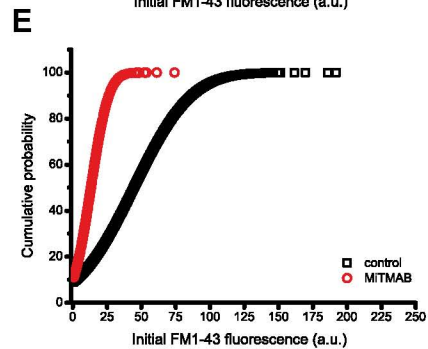
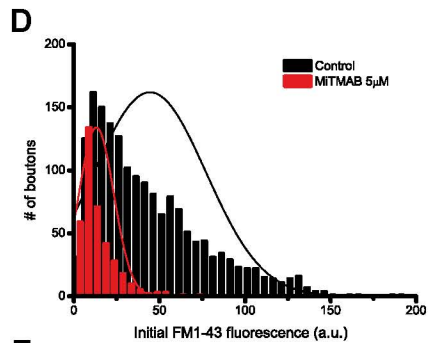
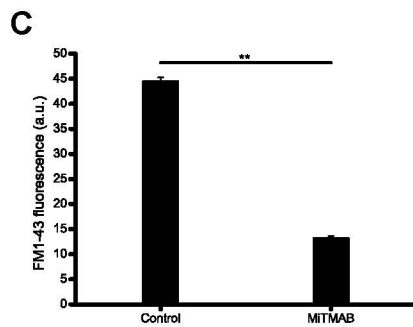
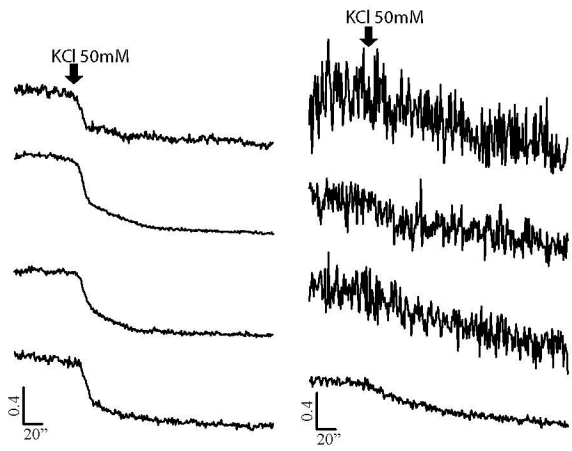


Fig. S2. Neuronal maturation of cerebellar granule cells involves an increase in the expression of synaptic proteins. (A) Solubilized extracts of cell cultures at 3, 7 and 14 DIV were resolved by SDS-PAGE (7.5% acrylamide) and analyzed by a standard Western blotting procedure. Quantification of dynamin, syntaxin, synaptojanin and synapsin expression normalized to the GAPDH or β -tubulin content in cerebellar granule cell cultures at 3, 7 and 14 DIV. (B) Histogram showing the mean (\pm SEM) protein content normalized to values at 3 DIV. n=3 experiments performed on different cultures. * $p \leq 0.05$, ** $p \leq 0.01$ when compared with values at 3DIV, t-test.

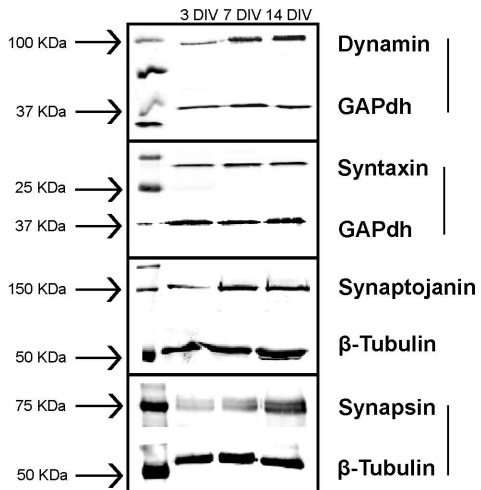
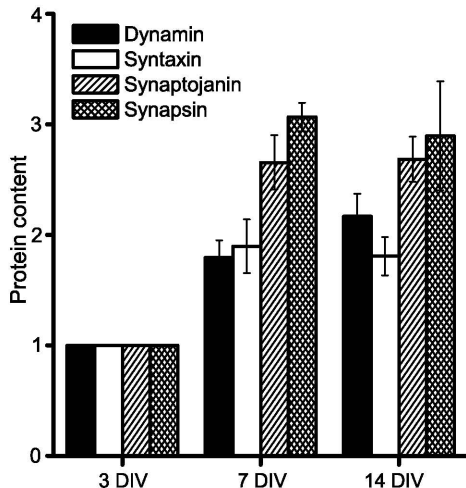
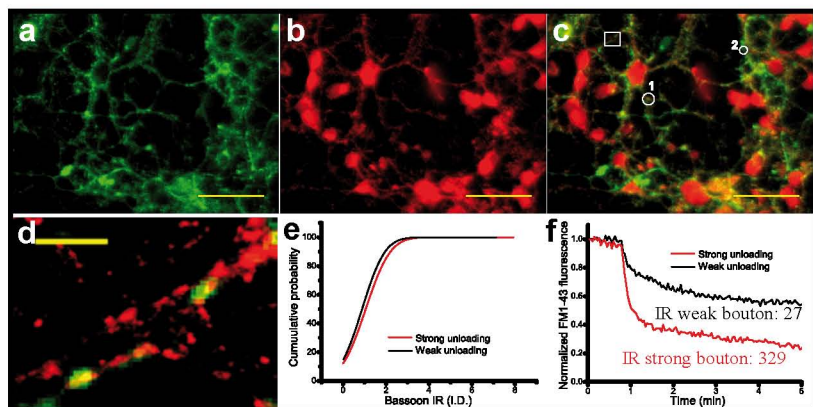
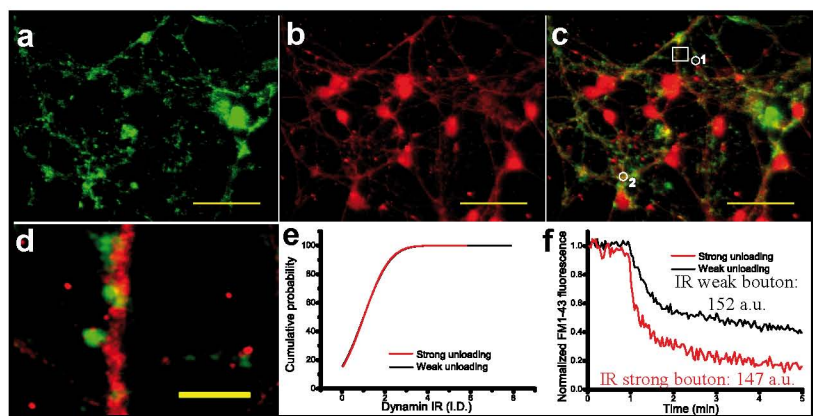
A**B**

Fig. S3. Synaptic boutons with strong FM1-43 unloading contain more bassoon and munc13-1 than the nerve terminals with weak FM1-43 unloading. The expression of dynamin and vGlut1 is similar between the two groups of nerve terminals. (a) FM1-43 image, (b) immunofluorescence image, and merged FM1-43 and immunofluorescence images at low (c) and at high magnifications (d), (e) cumulative immunofluorescence of bassoon (A), dynamin (B), Munc13-1 (C) and vGlut1 (D) in nerve terminals with strong and weak FM1-43 unloading profiles. (f) An example of nerve terminals with strong and weak unloading kinetics (shown as 1 and 2 in panel c, respectively). Differences in protein immunoreactivity (IR) expressed as the normalized integrated density (ID) of the two synaptic bouton populations for bassoon (E), dynamin (F), Munc13-1 (G) and vGlut1 (H). Integrated densities were normalized to the mean value of each experiment. The results shown in E, F, G and H represent the means \pm s.e.m of at least three experiments. n.s. $p \geq 0.05$ and ** $p \leq 0.01$, when comparing nerve terminals with strong versus weak unloading profiles (t-test).

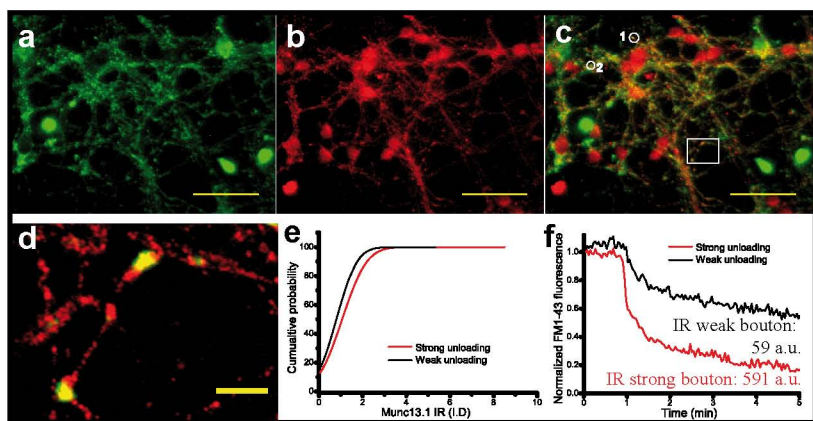
A



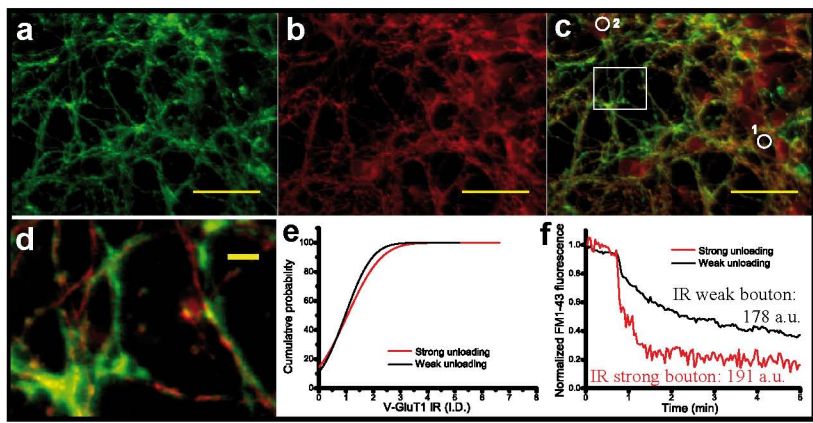
B



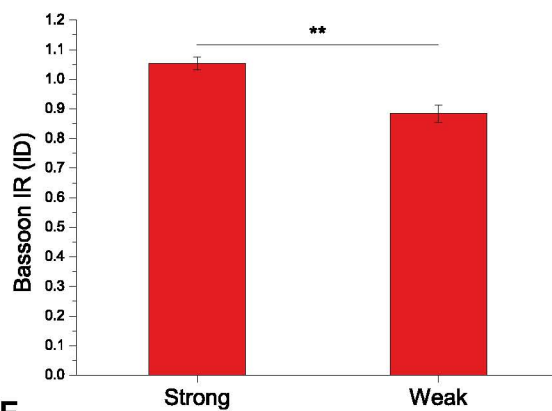
C



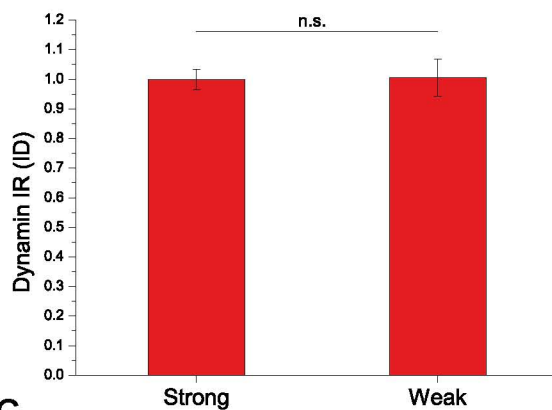
D



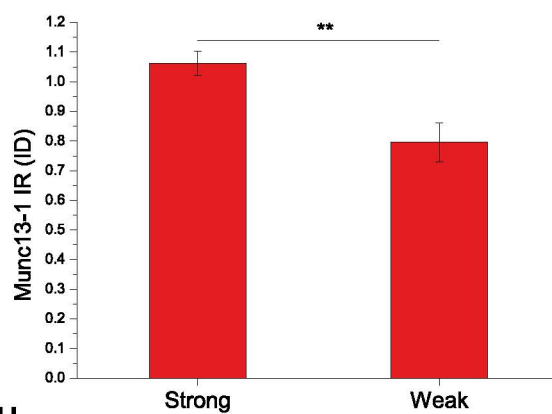
E



F



G



H

